An EMI Estimate for Shielding-Enclosure Evaluation

Min Li, James. L. Drewniak, *Member, IEEE*, Sergiu Radu, Joe Nuebel, Todd H. Hubing, *Senior Member, IEEE*, Richard E. DuBroff, *Senior Member, IEEE*, and Thomas P. Van Doren, *Senior Member, IEEE*

***Abstract*—A relatively simple, closed-form expression has been developed to estimate the EMI from shielding enclosures due to coupling from interior sources through slots and apertures at enclosure cavity modes. A power-balance method, Bethe's small-hole theory, and empirically developed formulas for the relation between radiation, and slot length and number of slots, were employed to estimate an upper bound on the radiated EMI from shielding enclosures. Comparisons between measurements and estimated field strengths suitably agree within engineering accuracy.**

***Index Terms*—Apertures, cavities, diffraction, electrical equipment enclosures, shielding.**

I. Introduction

IT IS DIFFICULT to meet EMC requirements for many high-speed digital electronic products without a shielding enclosure. The integrity of shielding enclosures is compromised by slots and apertures for heat dissipation, cable penetration, peripherals and displays. Radiation from slots and apertures in conducting enclosures, excited by interior sources, is of great concern in meeting radiated EMI requirements. In order to anticipate EMI problems with a shielded product, it is important to be able to estimate the effectiveness of the shielding enclosure.

Previous studies have found that cavity-mode resonances can result in significant radiation through electromagnetically short slots [1]. Radiation from conducting cavities at frequencies below cavity-mode resonances has been investigated experimentally and numerically [2]–[5]. Recent work determined the tangential electric fields from simulations and measurements, then applied equivalence principles to estimate the radiation from apertures [6]. The effect of aperture area on shielding effectiveness has also been studied [7]. A power balance method to estimate Qs of resonances associated with shielded enclosures has also been reported [8].

More recent efforts have studied an analytical formulation for the shielding effectiveness of an empty enclosure with apertures using an equivalent circuit for the shorted waveguide and aperture impedance [9], but only up to the fundamental cavity mode resonance. A calculation of the shielding effectiveness of rectangular enclosures with apertures by a modal expansion technique has also been reported [10]. Recent work reported in [11] investigated the influence of the aperture size, position, and number to the shielding effectiveness of a shielding enclosure. But the analysis was not concentrated on the shielding effectiveness at cavity-mode resonances. Much of the work done to date employs simulations that require significant computational resources and time, and may only be suitable for simple or ideal cases. This paper presents a relatively simple closed-form expression for estimating the radiated EMI from shielding enclosures as a worst-case envelope, instead of each individual cavity-mode resonance. Both analytical and empirical analyses are used. The application is for over-moded shielding enclosures at high frequencies. Many digital products, e.g., computers, are in this catagory.

An ideal rectangular cavity is first analyzed using a power balance method. The interior electronics are treated as a factor affecting the Qs of the shielding enclosure. Then, the slots are modeled as radiation sources using Bethe's small hole theory for slots less than $1/3\lambda$. Though the EMI estimate is based on a simple model, the comparison between the measurements and calculations is acceptable for engineering development.

II. Development of an EMI Estimate

A shielding enclosure has resonances associated with its dimensions. In practice, the exterior of shielding enclosures is often rectangular. However, the interior is broken up by circuit–board planes, plug-in modules, large heatsinks, sub-enclosures for power supplies, and other metal surfaces. These surfaces will affect resonance frequencies and cavity Qs. With so much complexity in the enclosure interior, these frequencies will shift in the course of the many changes that are a natural part of any design cycle. From an engineering perspective, however, predicting a specific resonance frequency is not necessary. An estimate of the envelope or upper bound of the radiation due to interior sources is desirable in engineering design in order to guide decisions on the use of EMI gaskets and screws, and the size and number of slots and apertures. The approach detailed below proceeds from simple cavity theory, making assumptions along the way regarding the modes, source, and cavity Q, which are based on measurements and numerical modeling.

The Bethe small-hole theory interprets the aperture as a radiating magnetic dipole $\vec{M}$ along the hole plane, and an electric dipole $\vec{P}$ along the direction normal to the hole plane [12]. The $\vec{M}$ and $\vec{P}$ are related to the short-circuited magnetic field in the hole plane $\vec{H}_0$, and the normal short-circuited electric field $\vec{E}_0$ as

$$\vec{M} = P_{\mathrm{m}}\vec{H}_0 \tag{1}$$

$$\vec{P} = P_{\mathrm{e}}\vec{E}_0 \tag{2}$$

Manuscript received January 10, 2000; revised April 10, 2001.

M. Li was with the University of Missouri, Rolla, MO 65409-0249 USA. She is currently with Lucent Technologies, Princeton, NJ 08542 USA.

J. L. Drewniak, T. H. Hubing, R. E. DuBroff, and T. P. Van Doren are with the Department of Electrical and Computer Engineering, University of Missouri, Rolla, MO 65409-0249 USA.

S. Radu and J. Nuebel are with Sun Microsystems, Palo Alto, CA 94303 USA.

Publisher Item Identifier S 0018-9375(01)07138-1.

where $P_{\rm m}$ and $P_{\rm e}$ are the magnetic and electric polarizabilities, respectively. The electric dipole does not contribute to the electric far field at observation points in front of the aperture panels. Then, the far field is given by

$$|E_{\rm far}| \simeq \eta \frac{\omega^2}{2\pi c^2 R} |\vec{M}|, \tag{3}$$

where η is the wave impedance, $\omega = 2\pi f$ ($f$frequency), c is the speed of light, and R is the distance between the source and observation point.

The magnetic polarizability for a slot with length L and width W can be found in the literature on microwave coupling as [13]

$$P_{\rm m} = \frac{0.132}{\ln(1+0.66\alpha)} L^3 \tag{4}$$

where α is the ratio of slot length L to slot width W. All units in this paper are in mks. The magnetic polarizability for a circular aperture is [14]

$$P_{\rm m} = \frac{4}{3} a^3 \tag{5}$$

where a is the radius of the circular aperture. According to (4) and (5), the magnetic polarizability of a square aperture is equivalent to that of a circular aperture with the same area within 0.7 dB . Bethe's expression for the radiated electric field in free space can then be augmented for small apertures with length L and width W as

$$|E_{\rm far}| = 8.8 \times 10^{-17} \frac{\omega^2 L^3 |H|}{\ln(1+0.66\alpha) R}. \tag{6}$$

An arbitrary interior field in an enclosure due to sources can be expanded in TM and TE modes for an ideal rectangular enclosure of width a, height b, and depth d. The distribution of interior fields and currents on the interior walls can be calculated for each cavity mode [8], [15]. The interior fields for a $TM_z(mnp)$ mode for an ideal rectangular cavity can be determined analytically [15]. The total energy W stored in a particular mode is related to the fields through the magnetic energy W_μ as

$$\begin{aligned} W =& 2W_\mu = 2\frac{\mu_0}{4} \int |\vec{H}|^2 dv \\ =& \frac{\mu_0}{2} \int_0^a \int_0^b \int_0^d \left(H_x^2 + H_y^2\right) dxdydz \\ =& A_{mnp}^2 n_g \frac{V}{8\mu_0} \left(\beta_x^2 + \beta_y^2\right) \end{aligned} \tag{7}$$

where $\beta_x = m\pi/a$, $\beta_y = n\pi/b$, $n_g = 1$ for $p = 0$, $n_g = 1/2$ for $p \neq 0$, $V = abd$ is the volume of the enclosure, and A_{mnp} is the modal coefficient.

The Q of an enclosure is defined as the ratio of time-averaged energy stored in the cavity, to the energy dissipated in the enclosure in one period. The stored energy W is related to the Q through

$$W = \frac{P_0 Q}{\omega} = A_{mnp}^2 n_g \frac{V}{8\mu_0} \left(\beta_x^2 + \beta_y^2\right) \tag{8}$$

where P_0 is the power delivered to the enclosure. The constant A_{mnp} can then be determined. For a slot along the x direction in the face $z = 0$ or $z = d$, the short-circuited field contributing to the radiation measured in front of the face containing the slot is H_x, and

$$H_x = \frac{A_{mnp}\beta_y}{\mu_0} = \left[\frac{8P_0 Q}{n_g \mu_0 \omega V \left(\frac{\beta_x^2}{\beta_y^2} + 1\right)}\right]^{1/2}. \tag{9}$$

The far-field radiation at distance R using (6) and (9) is then

$$|\vec{E}|_{\rm far} \simeq \frac{2.5 \times 10^{-16} \omega^{3/2} L^3}{\ln(1+0.66\alpha) R} \left[\frac{P_0 Q}{n_g \mu_0 V \left(\frac{\beta_x^2}{\beta_y^2} + 1\right)}\right]^{1/2}. \tag{10}$$

With the number of slots N included empirically (justified in a later section) and expressed as a function of frequency, f, the approximate far electric field is

$$|E_{\rm far}| = N \frac{3.9 \times 10^{-15} L^3 f^{3/2}}{\ln(1+0.66\alpha) R} \left[\frac{P_0 Q}{n_g \mu_0 V \left(\frac{\beta_x^2}{\beta_y^2} + 1\right)}\right]^{1/2}. \tag{11}$$

Assuming all of the available power is delivered to the enclosure, i.e.,

$$P_0 = \frac{V_{\rm s}^2}{8R_{\rm s}} \tag{12}$$

where $V_{\rm s}$ is the noise voltage and $R_{\rm s}$ is the noise source resistance. Neglecting n_g and assuming the mode numbers β_x and β_y are close to each other, an estimate for EMI is

$$|E_{\rm far}| \simeq \frac{1.2 \times 10^{-12} N V_{\rm s} L^3 f^{3/2}}{\ln(1+0.66\alpha) R} \sqrt{\frac{Q}{R_{\rm s} V}}. \tag{13}$$

At $R = 3$ m, with all terms expressed in mks units, the estimate can be expressed in the simplified form of

$$|E_{\rm far}| = 4.0 \times 10^{-13} \frac{N V_{\rm s} L^3 f^{3/2}}{\ln(1+0.66\alpha)} \sqrt{\frac{Q}{R_{\rm s} V}}. \tag{14}$$

At $R = 3$ m, (14) is an estimate for the envelope of radiated EMI from an enclosure that includes the frequency dependence, number of slots or apertures, perforation dimensions, enclosure volume and Q, and the source properties. The location, polarization, and dimensions of the source are not specified because an approximate worst-case envelope independent of these factors is sought. Hence, all of the available power from the source is used. At resonances, this is a reasonable worst-case approximation [1]. Equation (14) can also be given in terms of shielding effectiveness. Assuming a short linear dipole with current I as a noise source in the enclosure, (13) is calculated using the radiated power from the short dipole as available power. The resulting shielding effectivenss is then

$$\text{SE} = 1.2 \times 10^{12} \frac{\sqrt{\frac{V}{Q}} \ln(1+0.66\alpha)}{N L^3 f^{3/2}}. \tag{15}$$

The dependence on the number and dimensions of the slots (or apertures) is demonstrated using measurements and method of moment (MoM) modeling in the next section. A typical range of values for the enclosure Q was also determined

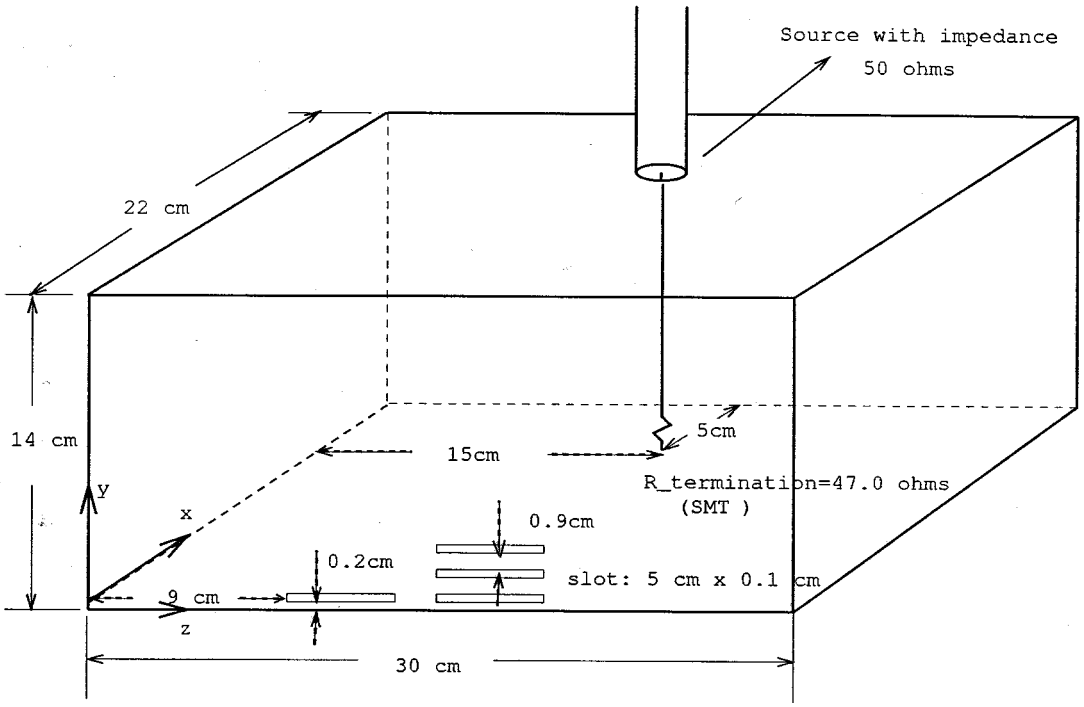

Fig. 1. Geometry of the small-test enclosure.

using a production populated printed circuit board (PCB) in an enclosure. The noise-source voltage V_s and the real part of the source impedance R_s depend on the type of source that is driving the enclosure resonance. An EMI estimate identical to that in (13) can also be developed for *TE* modes.

III. Corroborating and Applying the EMI Estimate

The factors for N (the number of slots or apertures), Q, L (the slot length), and the absence of terms for the source size, polarization and location in (13) require further justification. Both measurements and numerical modeling were used for this purpose. The EMI estimate was then applied to a testbed designed to approximate a SUN S-1000E server that included the motherboard and plug-in modules in the enclosure interior. Swept-frequency measurements with a known source were made to demonstrate the utility of this approach.

Two test enclosures were studied. One was a 22 cm$\times$14 cm $\times$30 cm cavity excited by a feed probe terminated with a 47-Ω resistor, as shown in Fig. 1. The resistor was introduced to provide the necessary loss for FDTD modeling. The other enclosure was a a 40 cm$\times$20 cm $\times$50 cm enclosure that mimicked the dimensions of a Sun S-1000E server, as shown in Fig. 2. A patch source driven against the top of the enclosure was used to approximate a noise source driving a heatsink in the real product, which was determined to be the primary coupling path for CPU harmonics [16]. In the functioning S-1000E, the perforations in the side panels were small-hole airflow aperture arrays that did not contribute appreciably to the radiated EMI, and the top and bottom had no perforations. Front- and back-panels were constructed for the S-1000E type test enclosure, as shown in Fig. 3, to study various aspects of the EMI estimate (13). Radiated EMI measurements were then made broadside to the front and back faces.

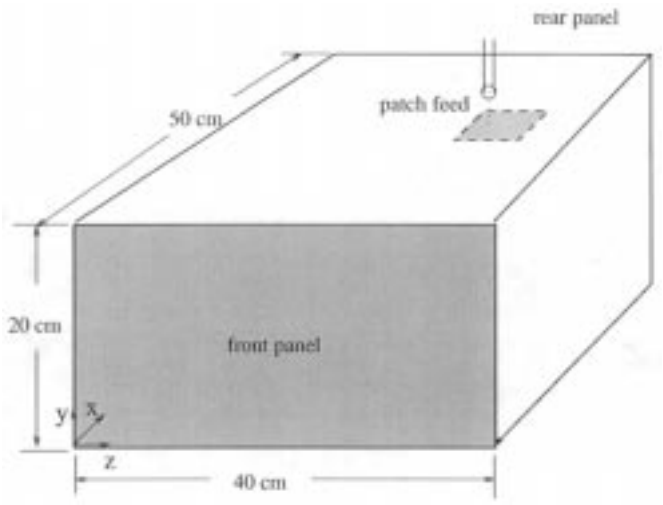

Fig. 2. Geometry of the test enclosure approximating the S-1000E enclosure.

Two-port S-parameter measurements made in a semi-anechoic chamber, where the source in the enclosure under test was connected to Port 1 of a Wiltron 37 247A network analyzer, and a horn antenna outside the enclosure was connected to Port 2. Measurements were made at 3 m, which is effectively the far-field at the frequencies of the enclosure resonances. The network analyzer was placed outside the semi-anechoic chamber and configured to measure the reflection coefficient $|S_{11}|$, and the transmission coefficient $|S_{21}|$. The electric field was calculated from $|S_{21}|$ and the antenna factor AF of the antenna at 3 m as

$$|\vec{E}|_{\text{far}} = V_{\text{in}} \times |S_{21}| \times AF = \frac{1}{2} V_s \times |S_{21}| \times AF \qquad (16)$$

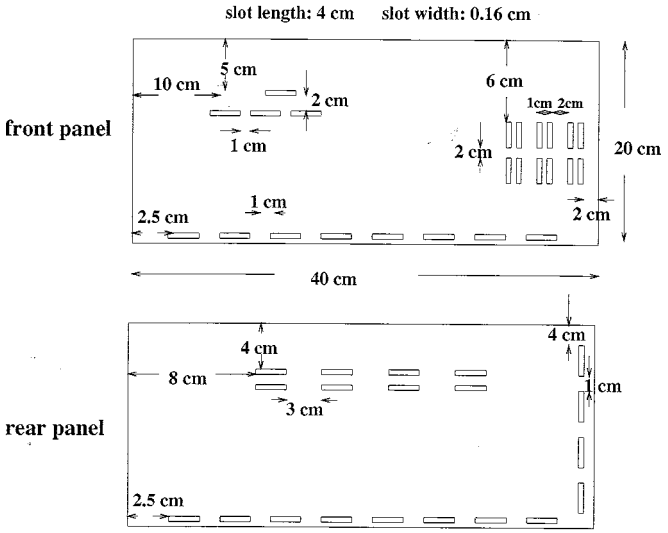

Fig. 3. The panels used in the S-1000E test enclosure with 4-cm slots as radiators.

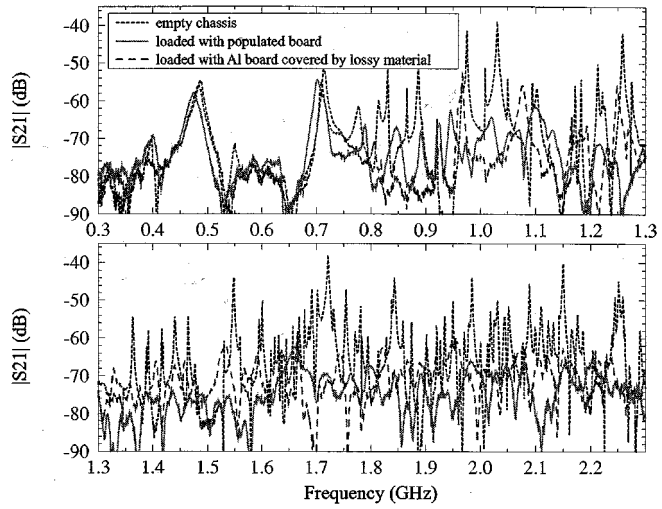

Fig. 4. The power delivered to the S-1000 test enclosure and EMI from the enclosure for different loading.

where V_{in} is the incident voltage at Port 1, which is half of the voltage source V_{s}, with a 50 Ω source impedance.

A. Quality Factor

The Q of the enclosure is an important factor in (13). The calculated field strength is proportional to the square root of Q, and an estimate of the Q for enclosures with interior electronics is needed in order to apply (13). Measurements of the S-1000E test enclosure were made both with and without a populated motherboard. An array of fifteen 4-cm long slots was located on the enclosure front and back faces as the radiators, as shown in Fig. 3. The measured value of $|S_{21}|$ corresponding to the electric field at 3 m is shown in Fig. 4. The Q was calculated from the radiated measurements as the ratio of a resonance frequency to the half-power bandwidth of that resonance. The Q at enclosure resonances for the empty test enclosure was as high as 1000. The Q for the test enclosure loaded with a populated motherboard ranged from 10 to 50 at resonances up to approximately 2 GHz.

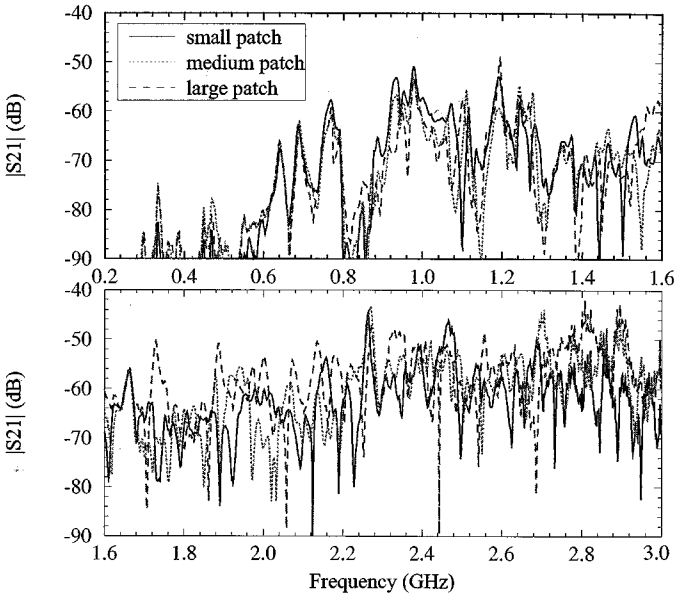

Fig. 5. The effect of patch size on $|S_{21}|$ (EMI) for the empty S-1000E test enclosure.

This demonstrates that loss due to circuitry inside the enclosure has a much greater effect on Q than the radiation loss. The authors' experience with other shielded products suggests that values of Q in the 10–50 range are typical.

The case of a shielding enclosure loaded with populated boards is assumed in this application. The impact of Q on the estimate in (13) is not as significant as the aperture and slot factors due to the square root. The Q ranging from 10 to 50 results in a difference of only 7 dB in the estimation. It can approximately be selected by how dense the boards are populated, and the board filling in the enclosure. For densely populated boards and a relatively full enclosure, a number close to ten should be used. For less populated boards, a number close to 50 is more reasonable.

A conductive lossy material (Milliken-110 $\Omega/\square$), 0.25-in thick, on an aluminum plane with the same size as the motherboard was utilized to mimic a PCB with electronics. The loading effect of the board covered with lossy material in the S-1000 test enclosure is similar to that of the populated S-1000 motherboard, as shown in Fig. 4. The lossy-material covered board is useful to mimic a populated PCB in enclosure evaluation before any electronics are available. This can be useful for numerical modeling, as well as experimental enclosure evaluation.

B. Source Characterization

The EMI estimate (13), is independent of the interior source size, polarization, and location. This assumption was tested experimentally. An arbitrary interior field can be expanded in terms of a complete set of enclosure modes, if the modes are known [14]. The modal coefficients of the expansion are determined by the inner product of the particular mode and the Maxwellian sources [14]. Consequently, the location, size, and polarization of the effective interior noise source driving the enclosure, or the "EMI antenna", will have a significant impact on the amplitude at any given resonance frequency.

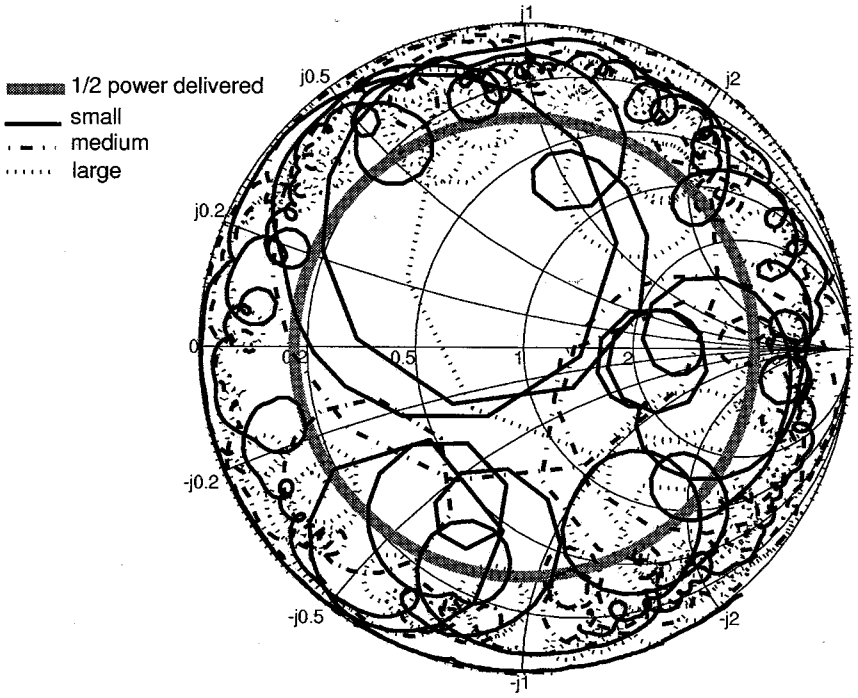

Fig. 6. The effect of patch size on input impedance for the empty S-1000E test enclosure.

Further, the location of the EMI antenna, e.g., a heatsink, is a boundary condition that affects the modal resonance frequencies. However, it is not practical to attempt to predict the amplitude of the radiated field at each resonance frequency. Instead, an estimate of maximum possible field as a function of frequency is desired.

Several source geometries—including a protruding monopole, circuit-board traces, and various size patches—were studied experimentally at numerous locations on three orthogonal enclosure walls. Three patch sizes—5 cm × 4 cm, 9 cm ×7 cm, and 15 cm × 10 cm,—were used as sources to determine the effect of patch size. The patches were intended to mimic heatsink sources, similar to those in the functioning S-1000E product. First, the patches were located on the $y = 20$ cm surface, at location (43, 20, and 33 cm), where the origin is specified as the left front corner, as depicted in Fig. 2. Each patch source was measured individually, and driven against the enclosure wall by a 3-cm long extension of a coaxial-cable feed probe connected to the patch. The enclosure was loaded with a populated motherboard, and the slot configuration was the same as shown in Fig. 3. The resulting $|S_{21}|$ measurements for the S-1000E test enclosure are shown in Fig. 5. The first few dominant resonance frequencies are relatively unaffected in frequency or amplitude by the patch size. When the patches are of significant dimensions relative to the wavelength, individual resonance frequencies and amplitudes change. However, overall, the EMI envelope for the different patch sizes is not appreciably different. Input-impedance measurements were also performed and are shown on the Smith Chart in Fig. 6. The thick gray circle indicates the half-power points. At frequencies where the impedance data fall inside the circle, the power delivered to the enclosure is more than half of the power available from the source. For each of the measured patch sizes, there were always a few enclosure resonances at which more than half of the power was delivered. Therefore, it is reasonable to assume that all of the available power is delivered to the enclosure when making a worst-case estimate.

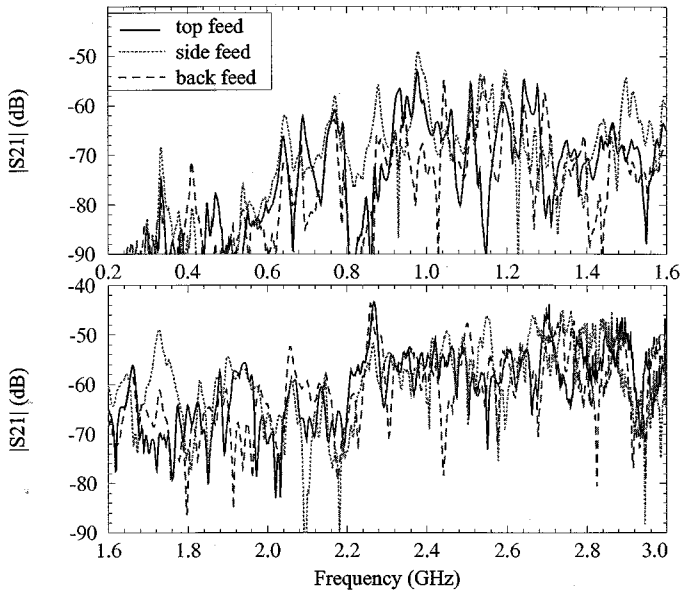

Fig. 7. The effect of different source positions on $|S_{21}|$ (EMI) for a 9 cm × 7 cm patch source exciting the S-1000E test enclosure.

The effect of different source positions and polarizations was also measured. Some of these results are shown in Fig. 7. The configuration is the same as above, except the 9 cm×77 cm patch source was located alternately on the top, side, and back walls (with respect to Fig. 2). For these measurements, a 25 cm ×20 cm one-sided unpopulated board was placed in the cavity 3 cm from the $y = 0$ wall. In all cases, the EMI envelope is

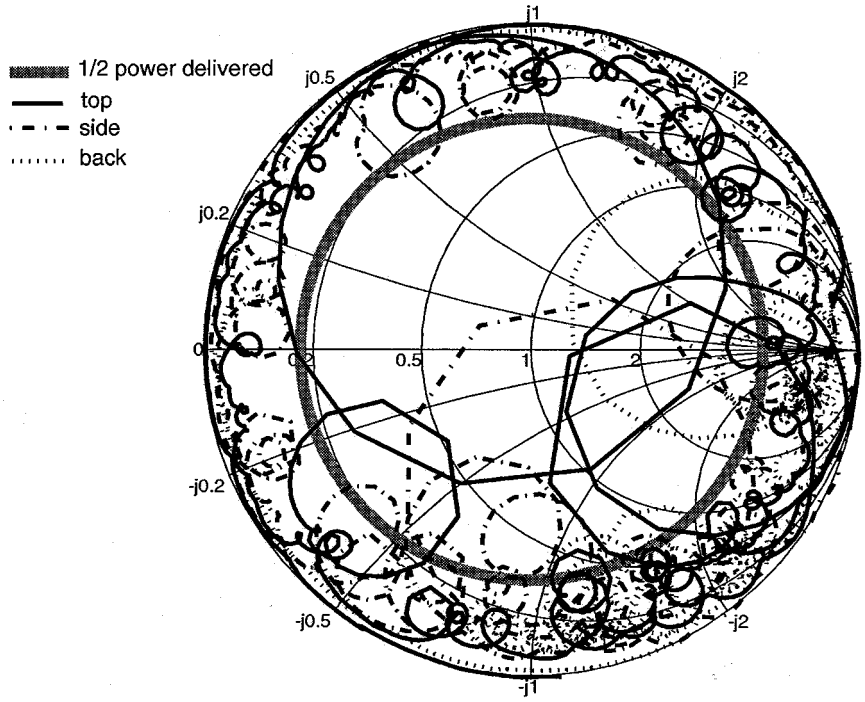

Fig. 8. The effect of different source positions on input impedance for a 9 cm × 7 cm patch source exciting the S-1000E test enclosure.

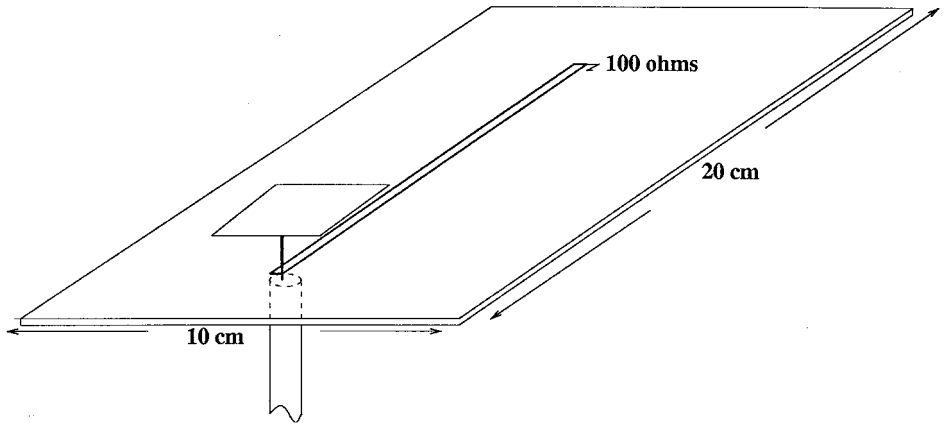

Fig. 9. Geometry for the transmission line, protruding wire, and patch used to excite cavity mode resonances in the small test enclosure.

approximately the same, though specific resonances may shift in frequency and amplitude. The input-impedance measurements are shown in Fig. 8. Again, there were always a few resonances at which more than half of the power was delivered for the three different patch positions.

Another source-related issue is the structure of the noise source. A transmission line (PCB trace), a protruding wire, and a protruding patch source, as shown in Fig. 9, were used individually to study the types of sources that may excite cavity mode resonances of an enclosure. The three different structures were driven against a 10 cm×15 cm circuit board located 2 cm above the $y = 0$ face in an otherwise empty test enclosure, as shown in Fig. 1. The wire EMI antenna was a monopole-type structure that extended 2 cm above the board's ground plane. The outer shield of the semi-rigid coaxial feed cable that penetrated the enclosure wall was soldered to the board's ground plane, and was also soldered to a copper tape square placed on the enclosure wall to establish a connection to the chassis wall. The patch EMI antenna was a 3 cm × 4 cm copper rectangle attached to the 2-cm protruding wire. The trace on the board was a 12-cm long transmission line with a 100-Ω characteristic impedance. The results of the radiated emissions measurements are shown in Fig. 10. The high-Q resonances are due to the unloaded empty chassis. The transmission line source is the least effective at driving the cavity, especially at frequencies below 1 GHz. In general, above 1 GHz, the radiated emissions are 50–20 dB below emissions due to the other two source structures. The 2-cm extended wire is as effective as the patch at frequencies above 1 GHz.

A conclusion of this study is that for practical EMC design, the amplitude of any given resonance is a strong function of the source shape, size, and location. However, once a potential noise source extends 1–2 cm above a circuit board, and has dimensions greater than approximately $1/10\lambda$, it may be an effective

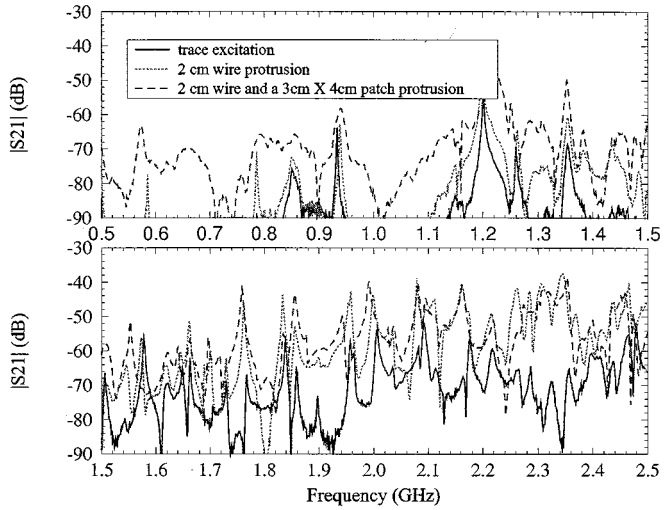

Fig. 10. The EMI resulting from the enclosure excitation by a transmission line, protruding wire, and patch in the small test enclosure.

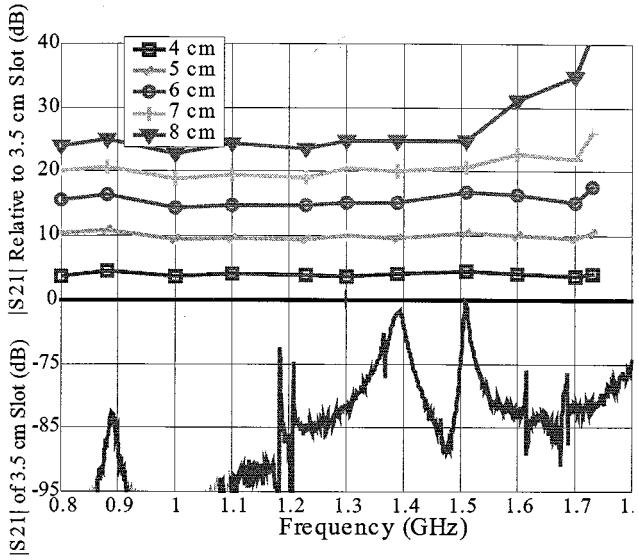

Fig. 11. The radiation from a single slot with varying slot length.

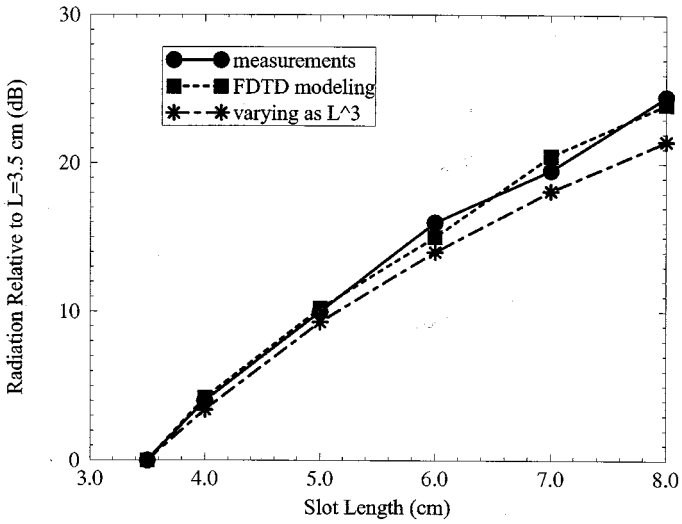

Fig. 12. The relation of EMI to slot length for a single slot.

source for driving the enclosure. At that point, the envelope of the radiation peaks does not shift up or down appreciably as a function of source geometry even though individual peaks do. Consequently, source location, size, and polarization are not included in the EMI estimate. This is fortuitous for practical applications, since the enclosure design is developed concurrently or prior to the interior electronics, and, further, the complexity of the interior irregularities makes predicting resonances difficult at best.

C. Slots and Apertures

The relation of (13) to the length and number of slots or apertures was studied experimentally, and modeled numerically. A single slot with varying slot length on the small test enclosure shown in Fig. 1 was investigated to demonstrate the L^3 relation between EMI and slot length. Measurements, as well as FDTD modeling, were employed, and the agreement was good, with a maximum difference of 2 dB for the far fields up to 2.2 GHz. The FDTD results are omitted in the following for clarity. The delivered power for slot lengths of 3.5, 4, 5 , 6, 7, and 8 cm was measured up to 1.8 GHz, and was not affected by the slot, except for the 8-cm slot, which is $1/3\lambda$ long at 1.2 GHz. The cavity modes are the coupling paths. The presence of an electrically short slot did not appreciably change the cavity-mode resonances. The $|S_{21}|$ measurements normalized to the 3.5-cm slot, as well as the $|S_{21}|$ of the 3.5-cm slot, are shown in Fig. 11. The shape of the radiation spectrum did not change appreciably with slot length. The increase in emissions at the first few resonances, TM_y101, TM_y111, and TM_y201 was approximately the same, which is summarized in Fig. 12 as a function of slot length. The curve for L^3 is normalized to the radiation from the slot with length 3.5 cm. The agreement is good, with the largest deviation being 2 dB for the 8-cm slot.

Equation (13) indicates that the EMI is directly proportional to the number of slots N. The application of this N-scale factor was investigated with measurements and numerical modeling. Measurements and FDTD modeling of two 5-cm slots end-to-end, and of two or three 6-cm slots side-by-side in the small test enclosure in Fig. 1 showed that the radiation from two slots was 6 dB (two times) greater than the radiation from a single slot. The radiation from three short parallel (side-by-side) slots was approximately 8.5 dB (approximately three times) greater than the radiation from a single slot, as shown in Fig. 13. Measurements of the S-1000E test enclosure for increasing numbers of 1 cm $\times$1 cm apertures in an aperture array (28 to 252 apertures) on one face also showed that the radiation was directly proportional to the number of apertures [17].

MoM modeling was also applied to investigate the mutual coupling between apertures and slots. The results indicate that the mutual coupling between apertures is generally insignificant if the spacing between apertures is not small compared to the aperture size [18]. The coupling between slots is also generally not important, for widely-spaced slots, e.g., the coupling between the three parallel slots in Fig. 13 results in only a 0.8-dB decrease from the N-factor application, and the coupling between the three serial slots results in a 0.3-dB increase.

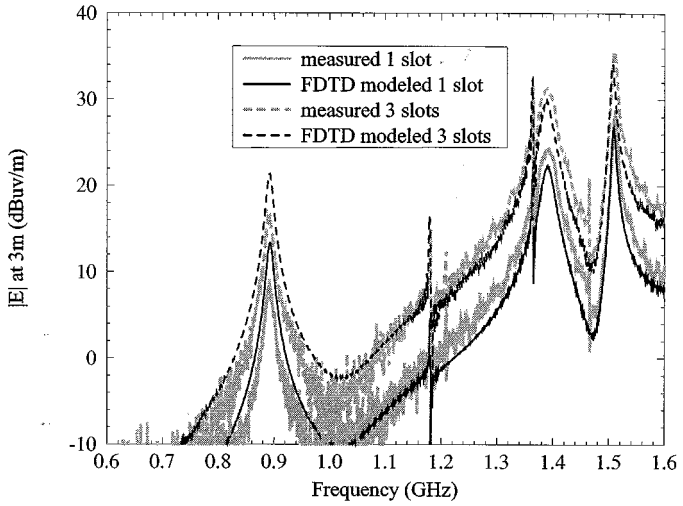

Fig. 13. The EMI from side-by-side multiple slots.

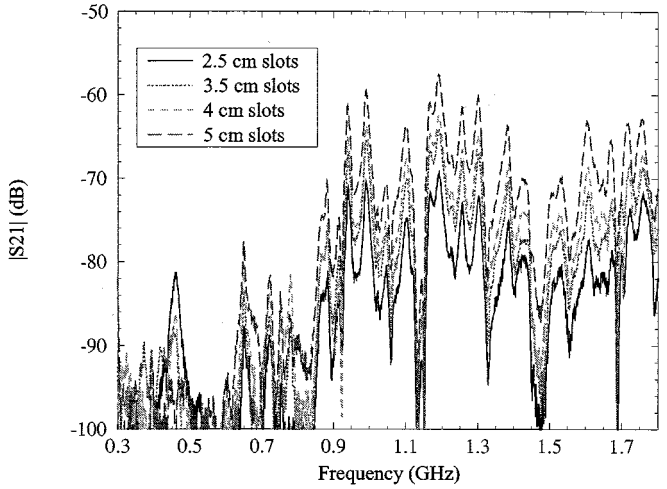

Fig. 14. Radiation from the S-1000E test enclosure excited by a patch source and loaded with the populated S-1000E motherboard.

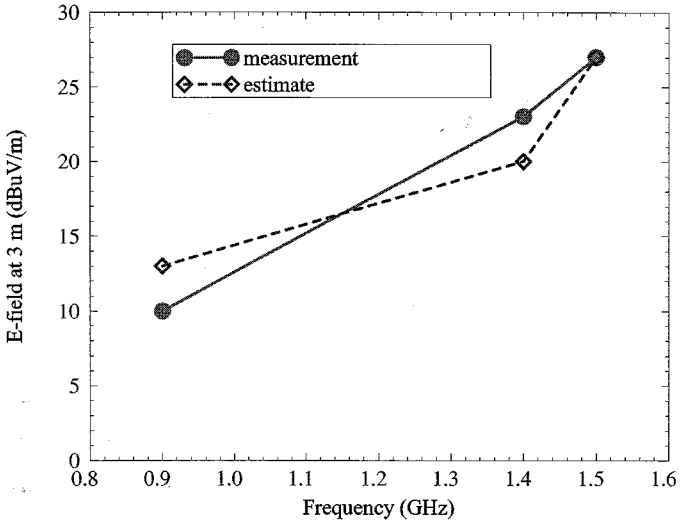

Fig. 15. Comparison of measurements and the EMI estimate for the small-test enclosure of Fig. 1 excited by a terminated source.

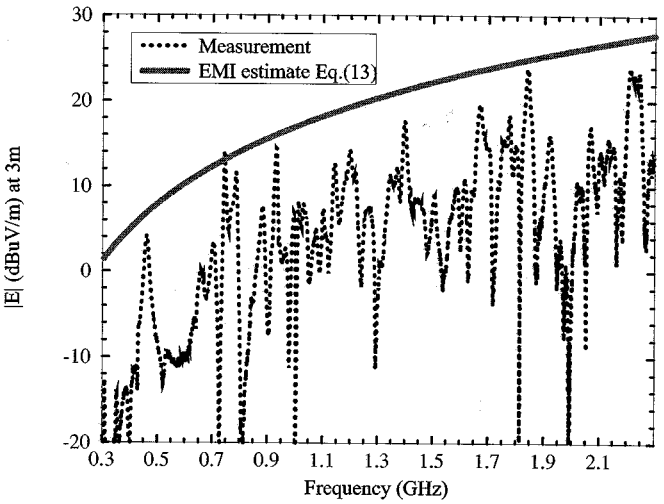

Fig. 16. Comparison of measurements and the EMI estimate for the S-1000E test enclosure excited by a patch source, with a populated motherboard in the interior.

The NL^3 factor was also tested for the S-1000 test enclosure. Fourteen 2.5-cm slots, ten 3.5-cm slots, eight 4-cm slots, and seven 5-cm slots were successively measured. The enclosure was excited by a patch source, and a populated S-1000E motherboard was placed in the interior. The measured $|S_{21}|$ with the receiving antenna facing the front panel is shown in Fig. 14. The increments in radiation from short slots to long slots were generally uniform at all frequencies, with an average value of 5 dB between the 2.5-cm slots and the 3.5-cm slots, 2 dB between the 3.5-cm slots and 4-cm slots, and 4 dB between the 4-cm slots and 5-cm slots. The increments varying as NL^3 would be 5.8, 1.5, and 4.6 dB. Again, the agreement is generally good.

D. Application

In order to test the applicability of the new EMI estimate, (13) was used to estimate the electric field at 3 m from the small enclosure shown in Fig. 1. The cavity was excited by a feed probe terminated with a 47-Ω resistor. The Q of the cavity resonances could be calculated for this simple case from the delivered power as the ratio of peak frequency to the half-power bandwidth. The source in this case is well-known, with a normalized $V_s = 1$ mV, and $R_s = 50\ \Omega$ for the network analyzer. The comparison between the esimate and measurement for the first three resonances is shown in Fig. 15. The agreement is good within 3 dB. Qs for the first three cavity-mode resonances are easily calculated from the $|S_{11}|$ measurements by the ratio of peak frequency to half-power frequency bandwidth. So an individual Q for each mode is used in the equation.

The S-1000E test enclosure excited with a patch source and loaded with the populated S-1000E motherboard was also tested. A comparison between measurements and the estimated field is shown in Fig. 16. Again, the source in this case was normalized to $V_s = 1$ mV, and $R_s = 50\ \Omega$ for the network analyzer. The Q used to calculate the EMI estimate curve was 15. Here, a global Q is used since the cavity-mode resonances are much more complicated than the case in Fig. 15. All factors in (13) were determined prior to plotting the EMI estimate, and there are no fitted parameters. The system was then measured

in a 3-m semi-anechoic chamber. The simple heuristically developed closed-form expression sufficiently predicted the envelope of the radiated field strength at enclosure resonances. Numerically modeling the complicated enclosure geometry including the populated motherboard in this situation, would not have been practical. However, the EMI estimate in (13) can be used to provide useful guidance for enclosure design.

IV. Summary and Conclusions

EMI from electrically short slots and small apertures results from the coupling of interior sources through enclosure cavity modes. Radiation from shielding enclosures through slots and apertures has been estimated using a simple heuristically determined closed-form expression, based on Bethe's small-hole coupling theory. The estimate explicitly accounts for the functional variation of EMI with frequency, number of apertures, size of apertures, enclosure volume, cavity Q, and the noise source voltage and resistance. Measurements and FDTD modeling were applied to develop and corroborate aspects of the estimate. Agreement between measurements (with a well-defined source) and the estimate was sufficient for application in engineering design.

The estimate has been developed based on electrically short slots, though it works reasonably well for $L < \lambda/3$. The demonstrated EMI variation with L can be used in design to reduce slot length to achieve a desired reduction in radiated EMI.

Although this estimate is a useful tool for designing and evaluating shielding enclosures, a shortcoming of this approach is the current lack of knowledge regarding the source properties V_s and R_s for the estimate. A common source that derives shielded enclosure resonances is an active IC that couples to a larger structure such as a heat sink. Models that can be used to estimate V_s and R_s for this type of source, and other coupling paths must be developed.

References

[1] M. Li, J. Nuebel, J. L. Drewniak, R. E. DuBroff, T. H. Hubing, and T. P. VanDoren, "EMI from cavity modes of shielding enclosures-FDTD modeling and measurements," *IEEE Trans. Electromagn. Compat.*, vol. 42, pp. 29–38, Feb. 2000.

[2] S. Daijavad and B. J. Rubin, "Modeling common-mode radiation of 3D structures," *IEEE Trans. Electromagn. Compat.*, vol. 34, pp. 57–61, Feb. 1992.

[3] S. Hashemi-Yeganeh and C. Birtcher, "Theoretical and experimental studies of cavity-backed slot antenna excited by a narrow strip," *IEEE Trans. Antennas Propagat.*, vol. 41, pp. 236–241, Feb. 1993.

[4] J. Y. Lee, T. S. Horng, and N. G. Alexopoulos, "Analysis of cavity-backed aperture antennas with a dielectric overlay," *IEEE Trans. Antennas Propagat.*, vol. 42, pp. 1556–1561, Nov. 1994.

[5] H. A. Mendez, "Shielding theory of enclosures with apertures," *IEEE Trans. Electromagn. Compat.*, vol. 20, pp. 296–305, May 1978.

[6] G. Cerri, R. D. Leo, and V. M. Primiani, "Theoretical and experimental evaluation of the electromagnetic radiation from apertures in shielded enclosure," *IEEE Trans. Electromagn. Compat.*, vol. 34, pp. 423–432, Nov. 1992.

[7] H. Y. Chen, I.-Y. Tarn, and Y.-J. He, "NEMP fields in side a metallic enclosure with an aperture in one wall," *IEEE Trans. Electromagn. Compat.*, vol. 37, pp. 99–105, Feb. 1995.

[8] D. A. Hill, M. T. Ma, A. R. Ondrejka, B. F. Riddle, M. L. Crawford, and R. T. Johnk, "Aperture excitation of electrically large, lossy cavities," *IEEE Trans. Electromagn. Compat.*, vol. 36, pp. 169–177, Aug. 1994.

[9] M. P. Robinson, T. M. Benson, C. Christopoulos, J. F. Dawson, M. D. Ganley, A. C. Marvin, S. J. Porter, and D. W. P. Thomas, "Analytical formulation for the shielding effectiveness of enclosures with apertures," *IEEE Trans. Electromagn. Compat.*, vol. 40, pp. 240–248, Aug. 1998.

[10] W. Wallyn, F. Olyslager, E. Laermans, D. D. Zutter, R. D. Smedt, and N. Lietaert, "Fast evaluation of the shielding effectiveness of rectangular shielding enclosures," in *Proc IEEE Electromagnetic Compatibility Symp.*, Denver, CO, 1998.

[11] F. Olyslager, E. Laermans, D. D. Zutter, S. Criel, R. D. Smedt, N. Lietaert, and A. D. Clercq, "Numerical and experimental study of the shielding effectiveness of a metallic enclosure," *IEEE Trans. Electromagn. Compat.*, vol. 41, pp. 202–213, Aug. 1999.

[12] H. A. Bethe, "Theory of diffraction by small holes," *Phys. Rev.*, vol. 66, pp. 163–182, 1944.

[13] N. A. McDonald, "Simple approximations for the longitudianl magnetic polarizabilities of some small apertures," *IEEE Trans. Microwave Theory Tech.*, vol. 36, pp. 689–695, July 1988.

[14] R. E. Collin, *Field Theory of Guided Waves*. Piscataway, NJ: IEEE Press, 1991.

[15] C. A. Balanis, *Advanced Engineering Electromagnetics*. New York: Wiley, 1989.

[16] S. Radu, Y. Ji, J. Nuebel, J. L. Drewniak, T. P. Van Doren, and T. H. Hubing, "Identifying an EMI source and coupling path in a computer system with sub-module testing," in *Proc. IEEE Electromagnetic Compatibility Symp.*, Austin, TX, 1997, pp. 165–170.

[17] M. Li, J. Nuebel, J. L. Drewniak, T. H. Hubing, R. E. DrBroff, and T. P. Van Doren, "EMI from airflow aperture arrays in shielding enclosures—experiments, FDTD, and MoM modeling," *IEEE Trans. Electromagn. Compat.*, vol. 42, pp. 265–275, Aug. 2000.

[18] M. Li, J. L. Drewniak, T. H. Hubing, and T. P. VanDoren, "Slot and aperture coupling for airflow aperture arrays in shielding enclosure designs," in *Proc. IEEE Electromagnetic Compatibility Symp.*, Seattle, WA, 1999, pp. 35–39.

Min Li was born in China, in 1968. She received the B.S. and M.S. degrees in physics (with honors) from the Fudan University, Shanghai, China, in 1990, and 1993, respectively, and the M.S. and Ph.D. degrees in electrical engineering from the University of Missouri, Rolla, in 1996, and 1999, respectively.

Since 1995, she has worked in the EMC lab at the University of Missouri, Rolla, Her research interests include numerical and experimental study of electromagnetic compatibility problems. She is currently with Lucent Technologies, Princeton, NJ.

Dr. Li has been the recipient of the Dean's Fellowship at the University of Missouri, and the winner of the 1998 IEEE EMC Society President Memory Award.

James L. Drewniak (S'85–M'90) received the B.S. (highest honors), M.S., and Ph.D. degrees in electrical engineering, all from the University of Illinois, Urbana-Champaign, in 1985, 1987, and 1991, respectively.

In 1991, he joined the Electrical Engineering Department at the University of Missouri, Rolla, where he is a Professor and is affiliated with the Electromagnetic Compatibility Laboratory. His research interests include the the development and application of numerical methods for investigating electromagnetic compatibility problems, packaging effects, and antenna analysis, as well as experimental studies in electromagnetic compatibility and antennas.

Sergiu Radu received the M.S. and Ph.D. degrees in electrical engineering (Electronics) from the Technical University of Iasi, Iasi, Romania.

He was an Associate Professor at the the Technical University of Iasi until 1996, involved in Electromagnetic Compatibility teaching and research. From 1996 to 1998, he was a Visiting Scholar at the University of Missouri, Rolla, as part of the Electromagnetic Compatibility Laborartory. In 1998 he joined the Electromagnetic Compatibility Engineering group, at Sun Microsystems, Inc., Palo Alto, CA, where he currently is a Senior Staff Engineer. He is also a NARTE certified engineer, and his research interests include electromagnetic compatibility aspects in high density, high-speed digital design, both at system level and chip or PCB level.

Joe Nuebel is currently a Staff EMC Engineer at Sun Microsystems, Palo Alto, CA. For over 15 years he has been working in the field of Electromagnetic Compatibility. His background also includes immunity, safety and networlk environment building systems (NEBS) testing for Telco. He also initiated university research at Sun in the area of EMC to assist in determining possible future EMC design concepts.

Todd H. Hubing (S'82–M'82–SM'93) received the B.S.E.E. degree from the Massachusetts Institute of Technology, Cambridge, in 1980, the M.S.E.E. degree from Purdue University, West Lafayette, IN, in 1982, and the Ph.D. degree in electrical engineering from North Carolina State University, Raleigh, NC, in 1988.

He is currently a Professor of electrical engineering at the University of Missouri, Rolla, where he is also a member of the principal faculty in the Electromagnetic Compatibility Laboratory. Prior to joining the faculty at the University of Missouri-Rolla in 1989, he was an Electromagnetic Compatibility Engineer at IBM, Research Triangle Park, NC. He has authored or presented more than 70 technical papers, presentations, and reports on electromagnetic modeling and electromagnetic compatibility-related subjects. He also writes the satirical "Chapter Chatter" column for the IEEE EMC SOCIETY NEWSLETTER. Since joining the UMR, the focus of his research has been measuring and modeling sources of electromagnetic interference.

Dr. Hubing is on the Board of Directors for the IEEE EMC Society.

Richard E. DuBroff (S'74–M'77–SM'84) received the B.S.E.E. degree from Rensselaer Polytechnic Institute, Troy, NY in 1970, and the M.S. and Ph.D. degrees in electrical engineering from the University of Illinois, Urbana-Champaign, in 1972 and 1976, respectively.

From 1976 to 1978, he held a postdoctoral position in the Ionosphere Radio Laboratory, University of Illinois, Urbana-Champaign, and worked on backscatter inversion of ionospheric electron density profiles. From 1978 to 1984, he was a Research Engineer in the geophysics branch of Phillips Petroleum, Bartlesville, OK. Since 1984, he has been affiliated with the University of Missouri, Rolla where he is currently a Profesor in the Department of Electrical and Computer Engineering.

Thomas P. Van Doren (S'60–M'69–SM'96) received the B.S., M.S., and Ph.D. degrees from the University of Missouri, Rolla in 1962, 1963, and 1969, respectively.

From 1963 to 1965, he served as an Officer in the U. S. Army Security Agency. From 1965 to 1967, he was a Microwave Engineer with Collins Radio Company, Dallas, TX. Since 1967, he has been a member of the electrical engineering faculty at the University of Missouri, where he is currently a Professor. His research interests concern developing circuit layout grounding, and shielding techniques to improve electromagnetic compatibility. He has taught short courses on electromagnetic compatibility to over 10 000 engineers and technicians representing 200 corporations.

Dr. Van Doren received the IEEE EMC Society Richard R. Stoddard Award for his contributions to electromagnetic compatibility research and education in 1995. He is a Registered Professional Engineer in the state of Missouri and a member of Eta Kappa Nu, Tau Beta Pi, and Phi Kappa Phi.